



Contents lists available at ScienceDirect

Peptides

journal homepage: www.elsevier.com/locate/peptides

Peptide corresponding to the C terminus of tissue factor pathway inhibitor inhibits mesangial cell proliferation and activation in vivo

Wang Liang^a, Juan Cheng^b, Rui Liu^a, Ji-ping Wang^a, Jin-gui Mu^a, Qing-hua Wang^c, Hui-jun Wang^d, Duan Ma^{a,d,*}

^aKey Laboratory of Molecular Medicine, Ministry of Education, Shanghai Medical College, Fudan University, Shanghai 200032, China

^bDepartment of Hematology, Shanghai Fifth People's Hospital, Fudan University, Shanghai 200240, China

^cDepartment of Medicine, University of Toronto, Ontario M5B 1W8, Canada

^dInstitutes of Biomedical Sciences, Fudan University, Shanghai 200032, China

ARTICLE INFO

Article history:

Received 25 June 2009

Received in revised form 21 August 2009

Accepted 21 August 2009

Available online xxx

Keywords:

Anti-proliferation

Apoptosis

C terminus

Mesangial cell

Proliferative glomerulonephritis

TFPI

ABSTRACT

Mesangial cells (MsCs) are one of the resident cell types in the glomerulus and are important with respect to its function and structure. The activation and proliferation of MsCs occur in several types of glomerulonephritis, particularly proliferative glomerulonephritis, producing a series of protein factors and matrix components that impair the normal structure and function of the glomerulus. To inhibit proliferation or induction of apoptosis is considered to be one mechanism that can be used to treat these diseases. In previous studies, we found that the tissue factor pathway inhibitor (TFPI) induces the apoptosis of cultured rat MsCs. Here, we expressed a series of TFPI fragments as fusion proteins to maltose binding protein (MBP-TFPI₁₆₂₋₁₈₈, MBP-TFPI₁₈₇₋₂₄₁, MBP-TFPI₂₄₀₋₂₇₆, MBP-TFPI₁₆₂₋₂₄₁, MBP-TFPI₁₈₇₋₂₇₆ and MBP-TFPI₁₆₂₋₂₇₆) and applied them to cultured rat mesangial cells. The C terminus of TFPI, a peptide corresponding to residues 240-276 of TFPI, was confirmed to induce apoptosis of MsCs in vitro. To observe the effect of this peptide on MsCs in vivo, we performed intramuscular gene transfer treatment on a rat model of proliferative glomerulonephritis with a plasmid containing the gene for the C terminus of TFPI. This revealed that the C terminus of TFPI exhibited suppressive effects on the activation and proliferation of MsCs and, thereby, improved renal function. Our data indicate that the C terminus of TFPI could be used in the treatment of proliferative glomerulonephritis.

© 2009 Published by Elsevier Inc.

1. Introduction

Mesangial cells (MsCs) play an important role in maintaining the structure and function of the glomerulus, including regulation of capillary flow, production of matrix components and cytokines, maintenance of the glomerulus structure and clearance of immune complexes and other macromolecules. However, MsCs also participate in the pathogenesis of many glomerular disorders by responding quickly to insults, in which the MsCs are activated and undergo proliferation, thus exhibiting an embryonic myofibroblastic phenotype. During this process, the mesangial matrix expands and abnormal components are produced. The production of cytokines and chemokines can stimulate proliferation and cause infiltration of inflammatory cells in the mesangium. All of these steps are involved in the mechanism by which the body fights noxious stimuli in the glomerulus [11,26].

However, in some situations, the MsC response is markedly elevated and continuous, producing abundant matrix. In such instances, the matrix differs from the normal one in terms of its components and structure [25]. Hypercellularity and extensive matrix deposition impair the structure and function of the glomerulus, resulting in glomerulosclerosis, which is involved in end-stage renal disease. This is particularly true in IgA nephropathy, mesangial proliferative glomerulonephritis, lupus nephritis and diabetic nephropathy [13,16,28].

Apoptosis and antiproliferative activity can inhibit hypercellularity in the mesangium, thus aiding the healing of glomerulonephritis [30,3]. In previous studies, we found that the tissue factor pathway inhibitor (TFPI), which consists of three tandem Kunitz-type domains (KD1, KD2 and KD3) and a highly basic C terminal, can induce apoptosis in cultured rat MsCs, whereas a truncated form of TFPI, TFPI₁₋₁₆₁, could not [20]. Accordingly, it seems that a structure comprised of KD3 and the C terminus is responsible for this effect, although the molecular mechanism is still unclear. In the present study, we expressed a series of TFPI fragments and treated serum-starved MsCs with these fragments. Overall, we found that the C terminus of TFPI is essential for inducing apoptosis.

* Corresponding author at: Fudan University, Key Laboratory of Molecular Medicine, Ministry of Education, BOX 238, 138# Yi Xue Yuan Road, Shanghai 200032, China. Tel.: +86 21 54237441; fax: +86 21 54237135.

E-mail address: duanma@shmu.edu.cn (D. Ma).

48 The anti-Thy1 nephritis rat model is a well established model
49 for researching mesangial proliferative glomerulonephritis char-
50 acterized by MsC proliferation and matrix expansion [19,1]. To test
51 the effect of the C terminus of TFPI on MsCs in vivo, we constructed
52 a plasmid expressing a gene for the C terminus of TFPI that was
53 fused to the human serum albumin signal peptide (HSA-SP), and a
54 control plasmid expressing only the HSA-SP gene. The plasmids
55 were transformed to muscle tissue via an electroporation-
56 enhanced intramuscular gene transfer method [18]. Using this
57 technique, we demonstrated that the C terminus of TFPI inhibits
58 the proliferation and activation of MsCs rather than apoptosis in
59 vivo. The renal function was also protected by the expression of the
60 C terminus of TFPI. These findings suggest the clinical usage of a
61 peptide corresponding to the C terminus of TFPI for the treatment
62 of proliferative glomerulonephritis (PGN).

63 2. Materials and methods

64 2.1. Expression and purification of the TFPI fragment

65 To identify the required structure that induces apoptosis in
66 cultured rat MsCs, we expressed a series of TFPI fragments (Fig. 1A)
67 with the pMAL™ Protein Fusion and Purification System from NEB.
68 Briefly, a gene for each fragment was amplified by PCR and inserted
69 into the pMAL-c2E vector (NEB) with EcoRI and HindIII endonu-
70 clease sites. The expression vector was transformed into compe-
71 tent *E. coli* TB1 cells to prepare the expression strain for each
72 fragment of TFPI. The expression strain was then cultured in rich
73 medium (1% tryptone, 0.5% yeast extract, 0.2% glucose, 0.5% NaCl
74 and 100 µg/ml ampicillin) at 37 °C in a shaking incubator
75 (250 rpm). When the OD₆₀₀ of the culture had increased to
76 ~0.8, isopropylthiogalactoside (IPTG) was added to the medium to
77 a final concentration of 0.5 mM to induce protein expression, and
78 the temperature was modified to 28 °C. Five hours later, the
79 bacteria were collected by centrifugation, washed, and resus-
80 pended in buffer 1 (20 mM Tris-HCl pH 7.4, 200 mM NaCl, 1 mM
81 EDTA) and frozen at -80 °C for several hours. The suspension was
82 then thawed at room temperature, sonicated, and centrifuged to
83 remove any inclusion bodies or other cell debris. The supernatant
84 was retained for the purification steps.

85 Affinity and ion-exchange chromatography methods were used
86 for protein purification. First, the supernatant was flowed through
87 an amylose resin column buffered with buffer 1. Then, the column
88 was washed with buffer 1 to record a baseline, and eluted with
89 elution buffer (buffer 1 + 10 mM maltose). The target fractions
90 were collected and dialyzed against buffer 2 (50 mM Tris-HCl pH
91 8.0, 1 mM EDTA) for 12 h at 4 °C. The desalted fraction was then
92 loaded on a Q-Sepharose Fast Flow (Amersham) column pre-
93 balanced with buffer 2. The column was washed with buffer 2 to
94 record a baseline and the proteins were divided by elution with an
95 increasing salinity gradient. The purified proteins were dialyzed
96 against phosphate buffer (PB, 20 mM, pH 7.4) and freeze dried.

97 2.2. Cell culture and apoptosis analysis

98 The rat MsCs used in this experiment had undergone 5-10
99 passages and were maintained in DMEM medium (GIBCO)
100 supplemented with 10% newborn calf serum (GIBCO), 100 units/
101 ml penicillin and 100 µg/ml streptomycin, at 37 °C in a 5% CO₂
102 incubator.

103 For the Hoechst 33258 assay, the cells were seeded on sterile
104 glass cover slips in six-well plates and grown in medium
105 containing 10% newborn calf serum to about 80% confluence,
106 and were made quiescent by serum starvation for 24 h. Batches of
107 quiescent cells were treated with individual fusion proteins at a
108 final concentration of 2 µM. Twenty-four hours later, the cells
109 were fixed, washed twice with phosphate-buffered saline (PBS),
110 stained with Hoechst 33258 staining solution (Beyotime) for 5 min
111 at room temperature, and observed under a fluorescence micro-
112 scope using a 4',6-diamidino-2-phenylindole (DAPI) filter. Apop-
113 tosis was determined according to the appearance of fragmented
114 or condensed nuclei.

115 For flow cytometry, cells were seeded in 10 cm dishes in
116 complete DMEM medium. At approximately 80% confluency, the
117 cells were washed and serum-starved for 24 h, and then exposed to
118 the appropriate concentration of experimental proteins (2 µM
119 of each protein for the comparison of apoptosis between MBP-
120 TFPI₁₈₇₋₂₇₆ and MBP-TFPI₂₄₀₋₂₇₆, or stepwise concentrations of 0.5,
121 1 and 2 µM for the quantitative analysis of the effect of MBP-
122 TFPI₂₄₀₋₂₇₆). After 24 h, adherent cells and floating cells were

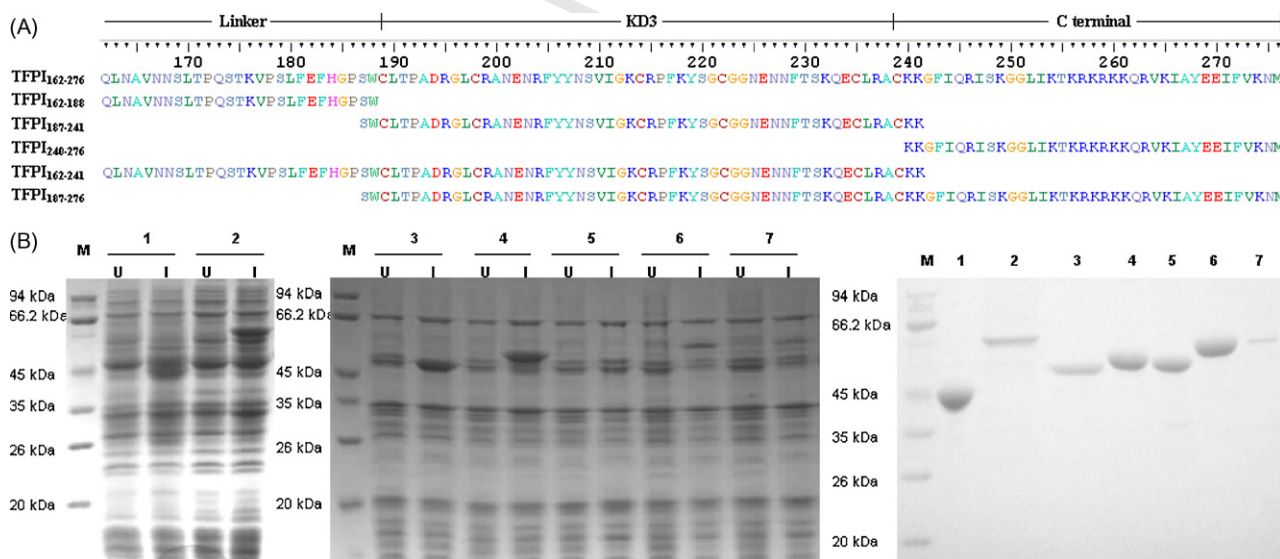


Fig. 1. Peptide design, expression and purification. (A) Domains and sequences of each TFPI fragment. This region was divided into three basic structures. The linker and C terminal are linear structures, and KD3 is a Kunitz-type domain. The fragments are composed of each structure or a combination. (B) Expression of fusion proteins in TB1 bacteria. (C) Purification of fusion proteins (M, protein marker; 1, MBP (expressed with the pMAL-c2E plasmid); 2, MBP-TFPI₁₆₂₋₂₇₆; 3, MBP-TFPI₁₆₂₋₁₈₈; 4, MBP-TFPI₁₈₇₋₂₄₁; 5, MBP-TFPI₂₄₀₋₂₇₆; 6, MBP-TFPI₁₆₂₋₂₄₁; 7, MBP-TFPI₁₈₇₋₂₇₆; U, uninduced; I, induced).

- 123 harvested. The collected cells were washed with PBS and fixed in
124 citric acid. The apoptotic ratio was analyzed by flow cytometry
125 with propidium iodide (PI) staining of the nuclei and was
126 performed at the Institute of Cell Biology (Shanghai, China).
- 127 **2.3. Electroporation-enhanced intramuscular gene transfer**
- 128 To evaluate the in vivo effect of the C terminus of TFPI on MsCs,
129 its gene was fused to the HSA-SP gene with an overlap PCR method
130 and was inserted in the vector VRnew with the EcoRV and BamHI
131 endonuclease sites. The product, referred to as VRnew-SP(HSA)-
132 TFPI₂₄₀₋₂₇₆, enables the secretory expression of the C terminus of
133 TFPI in muscle tissue. The control vector (VRnew-SP(HSA))
134 contains only the HSA gene. The validated plasmids were amplified
135 and dissolved in normal saline (NS) to 1 µg/µl.
- 136 Rats were anesthetized with pentobarbital sodium in NS (3%,
137 4 mg/100 g bodyweight) and hair was removed from both hind
138 legs with depilatory paste. The rats were then injected in both
139 tibialis anterior muscles with 100 µg of either the VRnew-SP(HSA)
140 or the VRnew-SP(HSA)-TFPI₂₄₀₋₂₇₆ plasmids, or with an equal
141 volume of vehicle. The needle was fitted with a plastic collar to
142 limit muscle penetration to approximately 2 mm. After DNA
143 injection, the local skin was covered with conducting gel. Muscle
144 electroporation was performed using electrodes fitted to a pair of
145 calipers. Eight pulses of 200 V/cm and pulse length of 20 ms were
146 delivered at 1 s intervals.
- 147 **2.4. Animal models**
- 148 Anti-Thy1 serum (ATS) was prepared as described by Chen et al.
149 [4]. Male Sprague-Dawley rats weighing 90–110 g were obtained
150 from the Shanghai Laboratory Animal Center of the Shanghai
151 Institutes for Biological Science. The body weight and breeding
152 condition were consistent for all rats. After being housed for 3 days,
153 24 animals were randomly allocated into four groups ($n = 6$). As
154 shown in Fig. 4A, the animals in group A received an injection of
155 normal serum on days 0 and 7, while animals in groups B–D were
156 injected with ATS to induce the anti-Thy1 nephritis model.
157 Electroporation-enhanced intramuscular gene transfer was per-
158 formed on days 1 and 8; groups A and B received NS, group C
159 received VRnew-SP(HSA) and group D received VRnew-SP(HSA)-
160 TFPI₂₄₀₋₂₇₆. Serum and 24 h urine samples were collected on days
161 0, 6 and 15. Animals were sacrificed at the end of day 15. For each
162 animal, the left kidney was excised and fixed in 10% formalin for
163 the pathology analysis. Urine creatinine and serum creatinine
164 levels were detected using an ADVIA 1650 automatic biochemistry
165 analyzer (Bayer Company). Creatinine clearance rate (Ccr) was
166 calculated based on urine volume, urine creatinine and serum
167 creatinine. Animal studies were conducted using a protocol
168 approved by the committee for the care and use of laboratory
169 animals of Fudan University.
- 170 **2.5. Glomerulus histopathology**
- 171 The kidney was fixed in 10% formalin, dehydrated and then
172 embedded in paraffin. Three-micrometer-thick sections were
173 stained with hematoxylin-eosin (HE) or periodic acid Schiff (PAS)
174 reagents. In each HE-stained section, 100 glomeruli were selected
175 randomly and classified into four grades according to the area of the
176 glomerulus showing mesangial hypercellularity and/or ECM deposi-
177 tion: grade 1, the proportion of mesangial hypercellularity and/or
178 ECM deposition was less than 25%; grade 2, over 25–50%; grade 3,
179 50–75%; grade 4, >75%. Total cell counts were performed in 50 near
180 or in equatorially crossed glomeruli in each section. The total cell
181 number divided by the total number of glomeruli in a group was
182 determined as the average cell number for the group. In PAS-stained
sections, deposition of ECM was confirmed by quantitative analysis
with Image-Pro Plus 6.0 software.
- 2.6. Immunohistochemistry**
- Sections were baked at 56 °C for 8 h, dewaxed and hydrated.
Antigens were retrieved by microwave-treatment in 0.01 M citrate
buffer (pH 6.0) for 20 min. After the sections had cooled to room
temperature, they were soaked in 3% hydrogen peroxidase for
30 min to quench endogenous peroxidase activity. The sections
were washed with Tris-buffered saline (TBS; 0.05 M, pH 7.6) three
times for 2 min per wash. Then, the primary antibody (mAb anti- α -
smooth muscle actin [SMA] or proliferating cell nuclear antigen
[PCNA], Boster) was added and the sections were placed in a
humidified cabinet and incubated at 37 °C for 1 h and then at 4 °C
overnight. After washing with TBS three times, the sections were
incubated with mouse/rabbit HRP-IgG (Gentech Company) at 37 °C
for 45 min and washed again with TBS. Positive staining was
visualized as a reaction to 3,3'-diaminobenzidine (DAB) for 40 s.
Subsequently, the sections were stained with hematoxylin for 20 s
and soaked in hot water (55 °C) for 3 s. The sections were then
dehydrated and covered with a glass cover slip.
- 2.7. Measurements and statistical analyses**
- The histopathology assessments were performed under a light
microscope by a researcher blind to the treatment groups. The
quantification of ECM in the mesangium and α -SMA staining was
determined with Image-Pro Plus 6.0 software from nine fields of
view at 200 \times . Statistical analyses were performed using SPSS 11.0
software. The changes in Ccr were analyzed by a mixed linear
regression analysis method. Histopathology grading was per-
formed using a rank-sum test and the differences in numbers of
total cells, PAS staining, PCNA-positive cells and α -SMA staining
were validated by LSD t -tests.
- 3. Results**
- 3.1. Expression and purification of TFPI fragments**
- All of the fusion proteins and a free maltose binding protein
were expressed after the expression induction with IPTG (Fig. 1B).
The molecular weight of each protein was confirmed by SDS-PAGE
analysis. The purity of each protein exceeded 95% (Fig. 1C).
- 3.2. The C terminus of TFPI induces MsC apoptosis in vitro**
- In the Hoechst 33258 assay detection, cells treated with MBP-
TFPI₁₆₂₋₂₇₆, MBP-TFPI₁₈₇₋₂₇₆ and MBP-TFPI₂₄₀₋₂₇₆ exhibited nuclear
condensation and fragmentation (Fig. 2D, G and I) whereas the MBP-,
MBP-TFPI₁₆₂₋₁₈₈-, MBP-TFPI₁₈₇₋₂₄₁- and MBP-TFPI₁₆₂₋₂₄₁-treated
cells showed none of these morphological changes (Fig. 2E, F and H).
Therefore, the TFPI₁₆₂₋₂₇₆, TFPI₁₈₇₋₂₇₆ and TFPI₂₄₀₋₂₇₆ fragments, but
not the TFPI₁₆₂₋₁₈₈, TFPI₁₈₇₋₂₄₁ or TFPI₁₆₂₋₂₄₁ fragments, induced
apoptosis in cultured MsCs. This suggests that the TFPI₂₄₀₋₂₇₆ region
of the C terminus of TFPI is required for apoptosis induction.
- However, to exclude a synergistic effect of the KD3 to C
terminus of TFPI, we compared the apoptosis ratio between MBP-
TFPI₁₈₇₋₂₇₆- and MBP-TFPI₂₄₀₋₂₇₆-treated MsCs using flow cyto-
metry. We found no statistical difference in the apoptosis ratio
between the MBP-TFPI₁₈₇₋₂₇₆- and MBP-TFPI₂₄₀₋₂₇₆-treated MsCs
(Fig. 3A). This means that the C terminus of TFPI is adequate for
apoptosis induction.
- We also examined the effect of the C terminus on MsCs using
flow cytometry, which revealed that MBP-TFPI₂₄₀₋₂₇₆ induces
apoptosis in a dose-dependent manner (Fig. 3B).

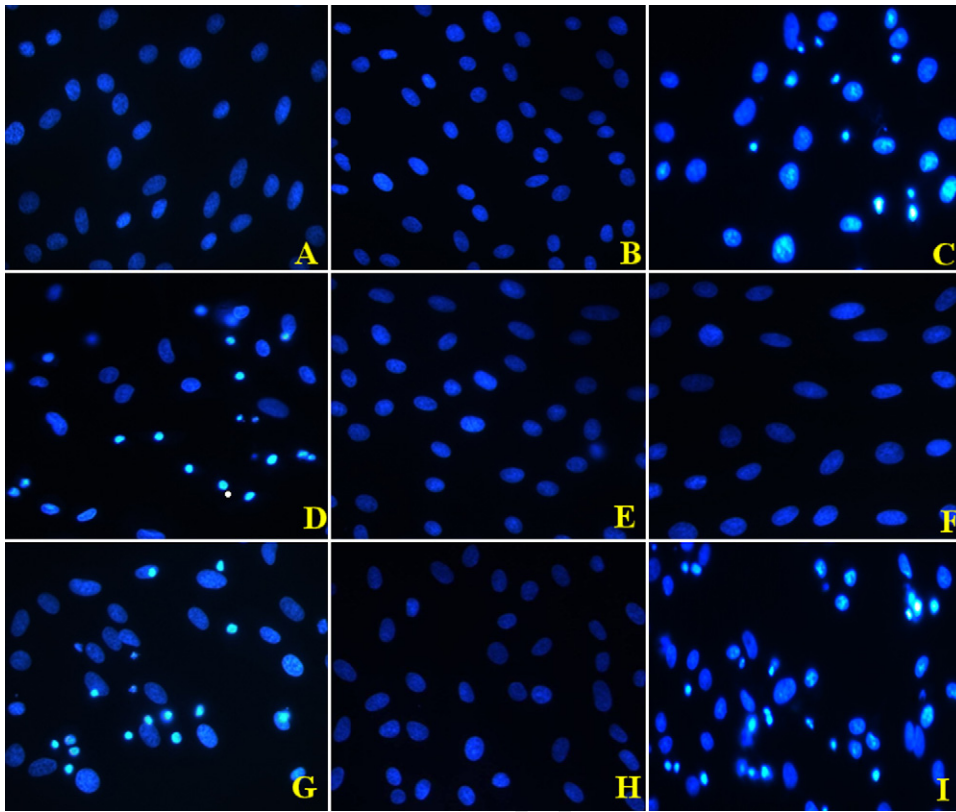


Fig. 2. Effects of fusion proteins on apoptosis of MsCs. Light blue spots indicate apoptotic cells. Each fusion protein was added to a final concentration of 2 μ M: (A) control (PB); (B) MBP; (C) rTFPI; (D) MBP-TFPI₁₆₂₋₂₇₆; (E) MBP-TFPI₁₆₂₋₁₈₈; (F) MBP-TFPI₁₈₇₋₂₄₁; (G) MBP-TFPI₂₄₀₋₂₇₆; (H) MBP-TFPI₁₆₂₋₂₄₁; (I) MBP-TFPI₁₈₇₋₂₇₆ (Hoechst 33258 staining, 400 \times).

3.3. Transgenic therapy with the C terminus of TFPI preserved renal function

Renal function is reflected by the value of Ccr. As shown in Fig. 4B, Ccr showed a natural increase as the body weight of each

rat increased by about 50 g each week. At the end of the study, the average bodyweight of each group was about 220 g; however, there were marked differences in Ccr between each group. The group treated with normal serum had the largest increment in Ccr (Δ Ccr = 1.8 ml/min) from days 0 to 15. By contrast, the increment in Ccr in the NS- and VRnew-SP (HSA)-treated groups was much smaller (Δ Ccr = 0.75 and 0.88 ml/min). The increment in Ccr in the VRnew-SP (HSA)-TFPI₂₄₀₋₂₇₆-treated group was partly restored (Δ Ccr = 1.28 ml/min), which indicates that transgenic therapy with the C terminus of TFPI improved renal function.

3.4. The C terminus of TFPI ameliorates glomerulus pathologies

In the histological study, the glomeruli of rats in groups B and C showed marked changes, including mesangial hypercellularity and ECM deposition on the hematoxylin-eosin-stained sections. By contrast, the glomeruli from group A were largely free of these changes. Group D, which was treated with the C terminus of TFPI, showed a significant decrease in the histological changes compared with group C (upper panel in Fig. 4C).

These changes in the glomeruli were evaluated semiquantitatively by grading and cell counting. Group B had a high proportion of glomeruli in grades 3 and 4 (44.3%), while that in group A was 6.4%; group C was lower than group B (31%); group D was markedly decreased to 19.7%. Furthermore, the proportion of grade 1 glomeruli was markedly increased in group D compared with group C (46.2% vs. 24.5%) (Fig. 4D). The total number of glomerular cells in group D was less than that in groups B and C (69.3 ± 1.15 vs. 79 ± 1.95 and 75.4 ± 1.05) (Fig. 4E). PAS staining revealed that ECM deposition was decreased in group D compared with groups B and C (0.51 vs. 0.57 and 0.56) (Fig. 4C(2) and F).

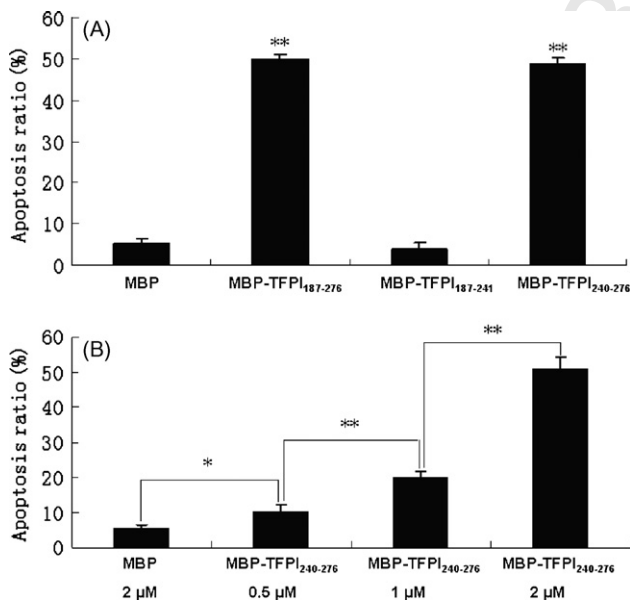


Fig. 3. The C terminus of TFPI induces apoptosis of cultured rat MsCs. (A) Apoptosis ratio of MsCs treated with 2 μ M of MBP-TFPI₁₈₇₋₂₇₆, MBP-TFPI₁₈₇₋₂₄₁ or MBP-TFPI₂₄₀₋₂₇₆ for 24 h; $**P < 0.01$ (compared with the MBP group). (B) MBP-TFPI₂₄₀₋₂₇₆ induces apoptosis in a dose-dependent manner; $**P < 0.01$, $*P < 0.05$. Data are expressed as means \pm SEM in parts A and B.

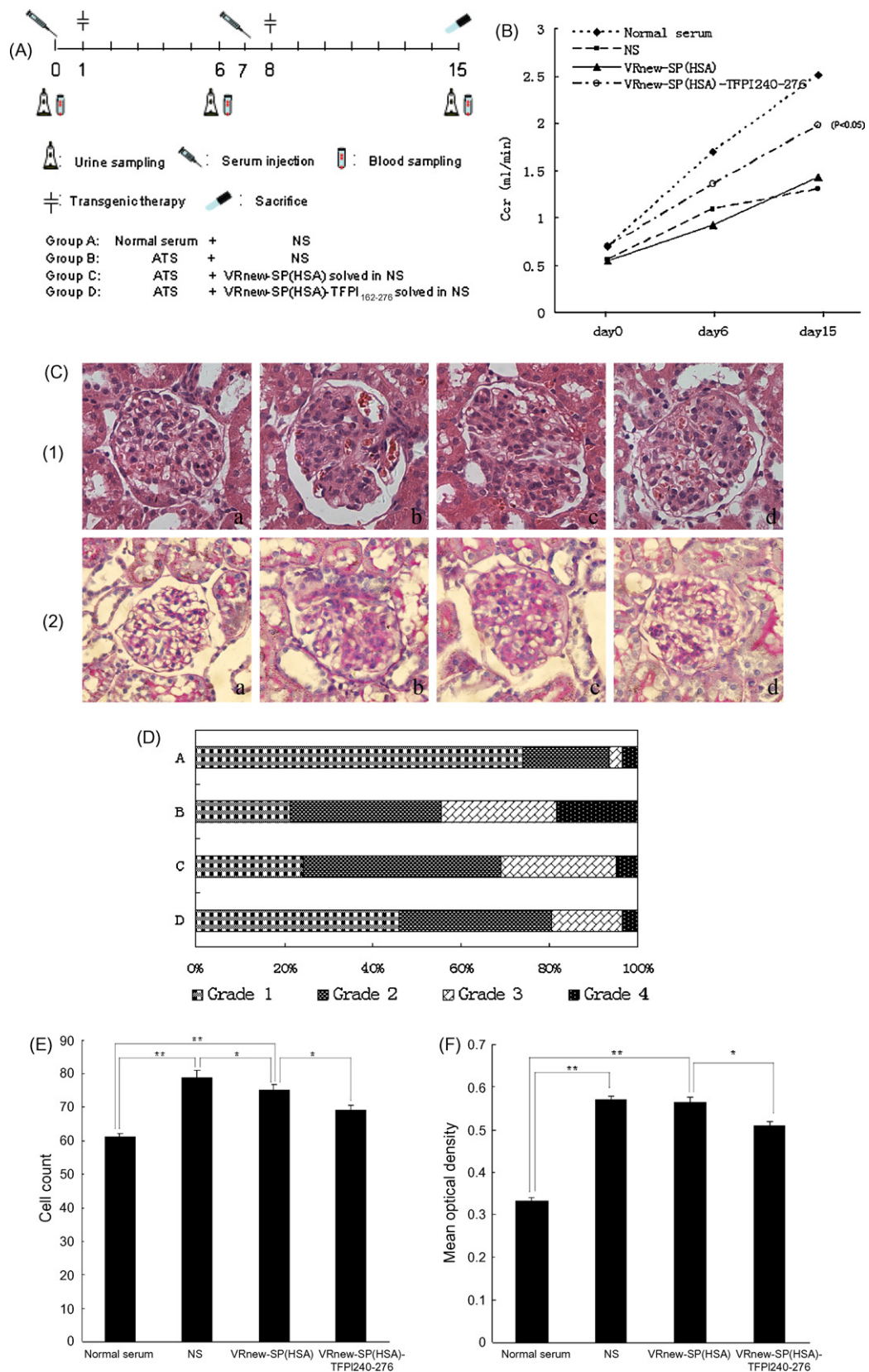


Fig. 4. The C terminus of TFPI ameliorates renal function and pathology in the anti-Thy1 nephritis model. (A) Induction of anti-Thy1 nephritis. Rats were intravenously injected with 500 μ l/100 g bodyweight of anti-Thy1 serum (ATS) (groups B–D) to induce the anti-Thy1 nephritis model. The control group (group A) was injected with normal rabbit serum. (B) The C terminus of TFPI maintained the progressive increase in creatinine clearance rate (Ccr). Urine and blood were sampled on days 0, 6 and 15. (C) Kidney glomerulus. Upper panel (1), HE staining (400 \times); lower panel (2), PAS staining (400 \times). Both panels, a: group A; b: group B; c: group C; d: group D. (D) The distribution of glomerular pathology grade was decreased in group D than in group C ($\chi^2 = 48.475$, $p = 0.0001$). (E) The total number of cells in the glomeruli from VRnew-SP(HSA)-TFPI₁₆₂₋₂₇₆-treated rats is less than that in the therapy control group. (F) ECM deposition in glomeruli mesangium was less in group D than in groups B and C. ****** $P < 0.01$, ***** $P < 0.05$. Data are expressed as means \pm SEM in (E) and (F).

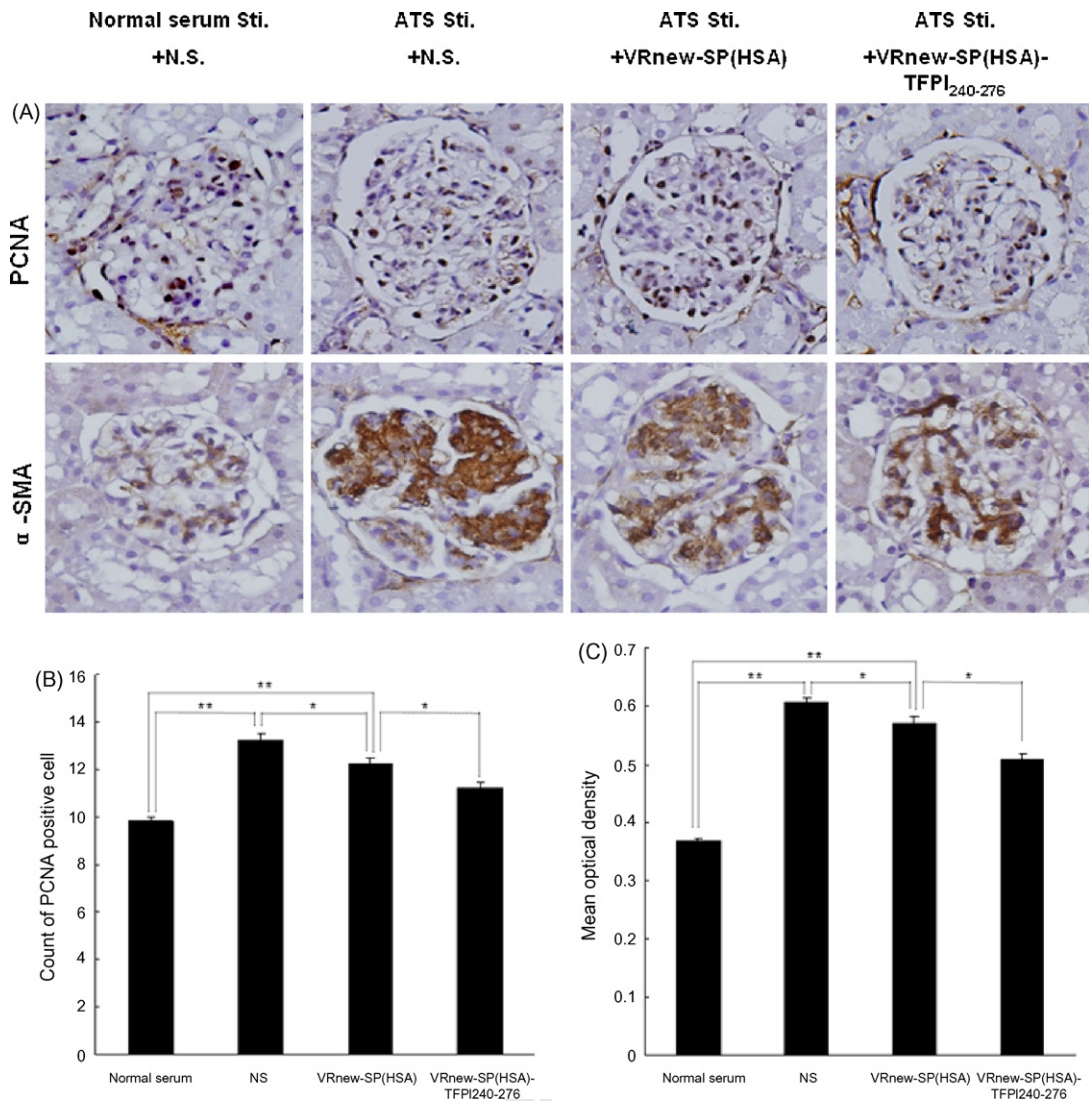


Fig. 5. The C terminus of TFPI attenuates mesangial cell proliferation and activation. The upper panel in (A) shows PCNA staining, the lower panel shows α -SMA staining (immunohistochemistry, 200 \times). The number of PCNA-positive cells (B) and the α -SMA staining intensity (expressed as the mean optical density in C) were decreased in the VRnew-SP (HSA)-TFPI₂₄₀₋₂₇₆-treated group. ** $P < 0.01$, * $P < 0.05$. Data are expressed as means \pm SEM in (B) and (C).

275 3.5. The C terminus of TFPI attenuates MsC proliferation and activation

276 In response to injury, MsCs change from the smooth muscle
277 phenotype to the embryonic myofibroblastic phenotype, and
278 express the cytoskeletal protein α -SMA, while PCNA is a biomarker
279 for cell proliferation. We detected the in situ expression of α -SMA
280 and PCNA via immunohistochemistry (Fig. 5A) to examine the
281 proliferation and activation of MsCs. We found that the mean
282 number of PCNA-positive cells in the glomeruli of rats in group D
283 was less than that in groups B and C (11.2 vs. 13.2 and 12.3)
284 (Fig. 5B). Similarly, the mean optical density of α -SMA staining in
285 the glomeruli was lower in group D than in groups B and C (0.51 vs.
286 0.61 and 0.57) (Fig. 5C). This suggests that the C terminus of TFPI
287 inhibited the proliferation and activation of MsCs in vivo.

288 4. Discussion

289 The function of the region of TFPI after the second Kunitz-type
290 domain appears to be complex. This region is less associated with its
291 anticoagulation effect but plays active roles in non-coagulation
292 bioactivity, by forming complexes with heparin, low-density
293 lipoprotein (LDL), lipopolysaccharide (LPS), low-density lipoprotein
294 receptor-related protein (LRP) or glycosaminoglycans (GAGs), which

induces the cellular binding, internalization of TFPI (or its complex)
or anti-inflammatory effect [2]. By creating truncated TFPI proteins,
our group, and others, have found that this region exerts an
antiproliferative or apoptotic effect on MsCs, human umbilical vein
endothelial cells (HUVECs) and vascular smooth muscle cells
(vSMCs) [17,9].

In the present study, we divided this region into several
fragments, which were fused with MBP, and expressed and
purified in a prokaryotic system. These proteins are soluble and
active, which enabled us to directly and comprehensively analyze
the effect of this region on MsCs. We found that the essential
structure that induces apoptosis in MsCs lies in the C terminus of
TFPI starting from residue 240. We have characterized the basic
sequence of this region and chemically synthesized the corre-
sponding polypeptide (LIKTKRKRKKQVRVIA). However, this poly-
peptide was unable to induce apoptosis in MsCs (data not shown).
This is consistent with the findings reported by Hembrough et al.,
who found that a peptide corresponding to residues 254-276 of
TFPI inhibited the proliferation of HUVECs by binding to VLDL,
while a sequence that was shorter than that synthesized by us was
able to maintain the VLDL-binding capacity but was unable to
inhibit the growth of HUVECs [10,27]. Because we have also
detected the expression of VLDL in MsCs (data not shown), we

295
296
297
298
299
300
301
302
303
304
305
306
307
308
309
310
311
312
313
314
315
316
317

hypothesized that TFPI induces apoptosis in MsCs by binding to VLDL, which is associated with the inhibition of the PI3-kinase/Akt pathway [20]. It seems that a complete C terminal peptide is essential for this process; however, characterization of the molecular mechanism requires further research.

We are also interested in whether this peptide can induce MsC apoptosis *in vivo* and whether it could be used in a clinical setting. To achieve these objective, we used intramuscular gene transfer treatment and found a baseline effect in the comparison between the NS- and VRnew-SP (HSA)-treated groups (Figs. 4D and E, 5B and C). However, our data confirmed that the C terminus of TFPI has an antiproliferative effect on MsCs. The number of PCNA-positive cells and the total number of cells in the glomeruli were decreased in the VRnew-SP (HSA)-TFPI_{240–276}-treated group compared with the control groups (NS or VRnew-SP (HSA)-treated). During proliferation, MsCs are activated and transformed to an embryonic myofibroblastic phenotype, as demonstrated by the increased expression of α -SMA [6,15]. Using immunohistochemistry, we found that the expression of α -SMA was decreased in the treated group compared with the control groups, which indicates that the C terminus of TFPI inhibited the activation of MsCs in glomerulonephritis. Notably, this phenomenon is deflected from that of the *in vitro* experiments for we have not detected apoptosis of MsCs in renal sections (data not shown), which might be due to lower expression efficiency and/or the complexity of the internal environment.

MsC proliferation results in hypercellularity in the glomerulus and, thus, enhanced production of active factors and abnormal matrix components such as collagen I and III to cause matrix expansion in the mesangium [14,24]. In our study, these histopathological changes were attenuated in the VRnew-SP (HSA)-TFPI_{240–276}-treated group, which might be due to the inhibition of proliferation and activation of MsCs by the C terminus of TFPI. Moreover, renal function was protected by treatment with the C terminus of TFPI. The Ccr on day 15 was markedly higher in the VRnew-SP (HSA)-TFPI_{240–276}-treated group than that in the control groups.

Clinical studies have revealed that TF and its inhibitor, TFPI, are expressed in glomeruli during glomerulonephritis, which implies that a balance between coagulation and anticoagulation is important in the development of glomerulonephritis [5,21,22]. Endothelial cells, mesangial cells and macrophages produce TF under stimulating conditions. TF increases the activation of FX by FVIIa, and the resulting product causes fibrin deposition and proliferation of resident cells [12,23]. Via inhibition of TF and FXa, TFPI was shown to reduce fibrin deposition, proteinuria and renal impairment in a rabbit crescentic glomerulonephritis model [7]. However, an *in vivo* effect of TFPI on mesangial cells has not been described until now. We suggest that TFPI exerts an antiproliferative effect on resident cells in the glomerulus either directly via its C terminus or indirectly through the inhibition of FXa, which benefits the turnover of glomerulonephritis.

Because the induction of apoptosis of resident cells is important in the treatment of PGN and because proliferation of MsCs and/or endothelial cells is a frequent phenomenon in these diseases [8,29], we believe that administration of the C terminus of TFPI, which is more readily available and has less effect on coagulation (particularly at high doses) than full-length TFPI, could be used in the treatment of PGN.

Acknowledgements

This research was supported by National 863 project (2006AA02Z109) and the National Basic Research Program of China (2009CB941704). We thank Prof. Zhi gang Zhang and Dr. Yi-feng Lin for their kindly direction. We also thank Yi-ming Li, Yi

Wang, Feng-yun Zheng, Cheng Xu and Hui-min Zheng for their help in the sample detection and data analysis.

References

- 1 Bagchus WM, Jeunink MF, Elema JD. The mesangium in anti-Thy-1 nephritis. Influx of macrophages, mesangial cell hypercellularity, and macromolecular accumulation. *Am J Pathol* 1990;137:215–23. 385
- 2 Bai H, Ma D, Zhang YG, et al. Molecular design and characterization of recombinant long half-life mutants of human tissue factor pathway inhibitor. *Thromb Haemost* 2005;93:1055–60. 386
- 3 Baker AJ, Mooney A, Hughes J, et al. Mesangial cell apoptosis: the major mechanism for resolution of glomerular hypercellularity in experimental mesangial proliferative nephritis. *J Clin Invest* 1994;94:2105–16. 387
- 4 Chen G, Guo M, Zhang Y-e. Preparation of anti-Thy1 serum and establishment of mesangioproliferative glomerulonephritis model in rat. *J Clin Exp Pathol* 1996;12:241–3. 388
- 5 Cunningham MA, Ono T, Hewitson TD, et al. Tissue factor pathway inhibitor expression in human crescentic glomerulonephritis. *Kidney Int* 1999; 55:1311–8. 389
- 6 El-Nahas AM. Plasticity of kidney cells: role in kidney remodeling and scarring. *Kidney Int* 2003;64:1553–63. 390
- 7 Erlich JH, Apostolopoulos J, Wun TC, et al. Renal expression of tissue factor pathway inhibitor and evidence for a role in crescentic glomerulonephritis in rabbits. *J Clin Invest* 1996;98:325–35. 391
- 8 Gómez-Guerrero C, Hernández-Vargas P, López-Franco O, et al. Mesangial cells and glomerular inflammation: from the pathogenesis to novel therapeutic approaches. *Curr Drug Targets Inflamm Allergy* 2005;4:341–51. 392
- 9 Hamuro T, Kamikubo Y, Nakahara Y, et al. Human recombinant tissue factor pathway inhibitor induces apoptosis in cultured human endothelial cells. *FEBS Lett* 1998;421:197–202. 393
- 10 Hembrough TA, Ruiz JF, Swerdlow BM, et al. Identification and characterization of a very low density lipoprotein receptor-binding peptide from tissue factor pathway inhibitor that has antitumor and antiangiogenic activity. *Blood* 2004;103:3374–80. 394
- 11 Herrera GA. Plasticity of mesangial cells: a basis for understanding pathological alterations. *Ultrastruct Pathol* 2006;30:471–9. 395
- 12 Hertig A, Rondeau E. Role of the coagulation/fibrinolysis system in fibrin-associated glomerular injury. *J Am Soc Nephrol* 2004;15:844–53. 396
- 13 Jia H, Qi X, Fang S, et al. Carnosine inhibits high glucose-induced mesangial cell proliferation through mediating cell cycle progression. *Regul Pept* 2009;154:69–76. 397
- 14 Johnson RJ, Floege J, Yoshimura A, et al. The activated mesangial cell: a glomerular “myofibroblast”? *J Am Soc Nephrol* 1992;2:S190–7. 398
- 15 Johnson RJ, Iida H, Alpers CE, et al. Expression of smooth muscle cell phenotype by rat mesangial cells in immune complex nephritis: alpha-smooth muscle actin is a marker of mesangial cell proliferation. *J Clin Invest* 1991;87:847–58. 399
- 16 Ka SM, Cheng CW, Shui HA, et al. Mesangial cells of lupus-prone mice are sensitive to chemokine production. *Arthritis Res Ther* 2007;9:R67. 400
- 17 Kamikubo Y, Nakahara Y, Takemoto S, et al. Human recombinant tissue-factor pathway inhibitor prevents the proliferation of cultured human neonatal aortic smooth muscle cells. *FEBS Lett* 1997;407:116–20. 401
- 18 Kumar M, Hunag Y, Glinka Y, et al. Gene therapy of diabetes using a novel GLP-1/IgG1-Fc fusion construct normalizes glucose levels in db/db mice. *Gene Ther* 2007;14:162–72. 402
- 19 Kumasaka R, Nakamura N, Fujita T, et al. Beneficial effect of neutrophil elastase inhibitor on anti-Thy1 1 nephritis in rats. *Nephrology (Carlton)* 2008;13:27–32. 403
- 20 Lin YF, Zhang N, Guo HS, et al. Recombinant tissue factor pathway inhibitor induces apoptosis in cultured rat mesangial cells via its Kunitz-3 domain and C-terminal through inhibiting PI3-kinase/Akt pathway. *Apoptosis* 2007;12:2163–73. 404
- 21 Lizakowski S, Zdrojewski Z, Jagodzinski P, et al. Plasma tissue factor and tissue factor pathway inhibitor in patients with primary glomerulonephritis. *Scand J Urol Nephrol* 2007;41:237–42. 405
- 22 Naumnik B, Borawski J, Chyczewski L, et al. Tissue factor and its inhibitor in human non-crescentic glomerulonephritis—immunostaining vs plasma and urinary levels. *Nephrol Dial Transplant* 2006;21:3450–7. 406
- 23 Nomura K, Liu N, Nagai K, et al. Roles of coagulation pathway and factor Xa in rat mesangioproliferative glomerulonephritis. *Lab Invest* 2007;87:150–60. 407
- 24 Patel K, Harding P, Haney LB, et al. Regulation of the mesangial cell myofibroblast phenotype by actin polymerization. *J Cell Physiol* 2003;195:435–45. 408
- 25 Poncelet AC, Schnaper HW. Regulation of human mesangial cell collagen expression by transforming growth factor- β 1. *Am J Physiol* 1998;275:F458–466. 409
- 26 Schocklmann HO, Lang S, Sterzel RB. Regulation of mesangial cell proliferation. *Kidney Int* 1999;56:1199–207. 410
- 27 Shirota I, Ikejima H, Kokame K, Hamuro T, et al. Tissue factor pathway inhibitor induces expression of JUNB and GADD45B mRNAs. *Biochem Biophys Res Commun* 2002;299:847–52. 411
- 28 Tamouza H, Vende F, Tiwari M, et al. Transferrin receptor engagement by polymeric IgA1 induces receptor expression and mesangial cell proliferation: role in IgA nephropathy. *Contrib Nephrol* 2007;157:144–7. 412
- 29 Tokuyama H, Kelly DJ, Cox A, et al. Tranilast ameliorates experimental mesangial proliferative glomerulonephritis. *Nephron Exp Nephrol* 2008;109:e1–7. 413
- 30 Watson S, Cailhier JF, Hughes J, et al. Apoptosis is and glomerulonephritis. *Curr Dir Autoimmun* 2006;9:188–204. 414